

# Carbon Exchange in an Amazon Forest: from Hours to Years

Matthew N. Hayek<sup>1</sup>, Marcos Longo<sup>2</sup>, Jin Wu<sup>3</sup>, Marielle N. Smith<sup>4</sup>, Natalia Restrepo-Coupe<sup>5</sup>, Raphael Tapajós<sup>6</sup>, Rodrigo da Silva<sup>6</sup>, David R. Fitzjarrald<sup>7</sup>, Plinio B. Camargo<sup>8</sup>, Lucy R. Hutyrá<sup>9</sup>, Luciana F. Alves<sup>10</sup>, Bruce Daube<sup>11</sup>, J William Munger<sup>11</sup>, Kenia T. Wiedemann<sup>11</sup>, Scott R. Saleska<sup>12</sup>, and Steven C. Wofsy<sup>11</sup>

<sup>1</sup> Harvard Law School, Cambridge, MA, United States

<sup>2</sup> NASA Jet Propulsion Laboratory, California Institute of Technology, Pasadena, CA, United States

<sup>3</sup> Biological, Environmental & Climate Sciences Department, Brookhaven National Lab, Upton, New York, NY, United States

<sup>4</sup> Department of Forestry, Michigan State University, East Lansing, MI, United States

<sup>5</sup> Plant Functional Biology and Climate Change Cluster, University of Technology Sydney, Sydney, NSW, Australia.

<sup>6</sup> Universidade Federal do Oeste do Pará, Santarém, PA, Brazil.

<sup>7</sup> University at Albany SUNY, Albany, NY, United States.

<sup>8</sup> Centro de Energia Nuclear na Agricultura, Universidade de São Paulo, Piracicaba, SP, Brazil.

<sup>9</sup> Department of Earth and Environment, Boston University, Boston, MA.

<sup>10</sup> Center for Tropical Research, Institute of the Environment and Sustainability, UCLA, Los Angeles, CA, United States.

<sup>11</sup> Faculty of Arts and Sciences, Harvard University, Cambridge, MA, United States.

<sup>12</sup> Department of Ecology and Evolutionary Biology, University of Arizona, Tucson, AZ, United States.

*Corresponding author:* Matthew Hayek (mhayek@law.harvard.edu)

**Abstract.** In Amazon forests, the relative contributions of climate, phenology, and disturbance to net ecosystem exchange of carbon (NEE) are not well understood. To partition influences across various timescales, we use a statistical model to represent eddy covariance-derived NEE in an evergreen Eastern Amazon forest as a constant response to changing meteorology and phenology throughout a decade. Our best fit model represented hourly NEE variations as changes due to sunlight, while seasonal variations arose from phenology influencing photosynthesis and from rainfall influencing ecosystem respiration, where phenology was asynchronous with dry season onset. We compared annual model residuals with biometric forest surveys to estimate impacts of drought-disturbance. We found that our simple model represented hourly and monthly variations in NEE well ( $R^2 = 0.81, 0.59$  respectively). Modeled phenology explained 1% of hourly and 26% of monthly variations in observed NEE, whereas the remaining modeled variability was due to changes in meteorology. We did not find evidence to support the common assumption that the forest phenology was seasonally light- or water-triggered. Our model simulated annual NEE well, with exception to 2002, the first year of our data record, which contained  $1.2 \text{ MgC ha}^{-1}$  of residual net emissions, because photosynthesis was anomalously low. Because a severe drought occurred in 1998, we hypothesized that this drought caused a persistent, multi-year depression of photosynthesis. Our results suggest drought can have lasting impacts on photosynthesis, possibly via partial damage to still-living trees.

## 1. Introduction

The Amazon's tropical forests are pivotal to global climate, exchanging large, globally important quantities of energy and matter, including atmospheric carbon (Betts et al., 2004). Amazon forests contain 10-20% of Earth's biomass carbon (Houghton et al., 2001). Increased emissions of the forest's carbon can therefore accelerate climate change and attention is now focused on how vulnerable this large reservoir of carbon will be to a potentially drier future climate (de Almeida Castanho et al., 2016; Farrior et al., 2015; Duffy et al., 2015; Longo et al., 2018; McDowell et al., 2018). Characterizing the response of present-day Amazon rain forest carbon balance to climate and drought disturbance is a necessary step to improving predictions of future vulnerability.

Eddy covariance  $\text{CO}_2$  flux measurements are a powerful tool for quantifying net ecosystem exchange of carbon (NEE) (Baldocchi, 2003). NEE is the difference between uptake from gross ecosystem productivity (GEP) and emission from

41 ecosystem respiration (RE). The magnitudes of these gross fluxes are influenced both by exogenous environmental conditions  
42 such as light, moisture, and temperature (Collatz et al., 1991; Bolker et al., 1998; Fatichi et al., 2014; Kiew et al., 2018), as well  
43 as endogenous biophysical properties such as canopy structure, phenology, and community composition (Barford et al., 2001;  
44 Melillo et al., 2002; Dunn et al., 2007; Doughty and Goulden, 2008; Stark et al., 2012; Frey et al., 2013; Morton et al., 2016; Wu  
45 et al., 2016).

46 Partitioning the exogenous and endogenous influences upon eddy covariance NEE is possible using statistical modeling  
47 (Barford et al., 2001, Yadav et al., 2010; Wu et al., 2017). To partition influences upon NEE in a 20-year eddy flux record in a  
48 temperate New England forest, Urbanski et al. (2007) used a statistical modeling approach: by representing hourly NEE merely  
49 as response to exogenous meteorology and annually integrating their results, they concluded that meteorology did not explain the  
50 accelerated uptake seen annually integrated NEE. They hypothesized that residual uptake was due to long-term forest regrowth  
51 and succession, a hypothesis that was corroborated by biometric measurements of increasing canopy foliage and accelerating  
52 mid-successional tree biomass accrual. This novel partitioning framework for NEE has not previously been applied to any  
53 tropical forest, in part because long-term eddy covariance coverage of tropical forests is lacking (Zscheischler et al., 2017). A  
54 simple statistical framework may allow tropical forest CO<sub>2</sub> flux measurements to better inform model development and  
55 improvement.

56 On seasonal timescales, tropical evergreen forests undergo endogenous changes in GEP via the phenology of leaf flush  
57 and abscission (Doughty and Goulden, 2008, Restrepo-Coupe et al., 2013; Wu et al., 2016). The seasonal dependency of  
58 productivity has motivated the development of rooting depth and phenology sub-models in DVGMs (Verbeeck et al., 2011; De  
59 Weirdt et al., 2012; Kim et al., 2012). These sub-models have led to complexity in the modeled mechanisms controlling the GEP  
60 seasonal cycle without necessarily improving accuracy. It is necessary to quantify the magnitude and timing of phenology's  
61 effect on the GEP seasonal cycle after accounting for the integrated hourly response to sunlight.

62 On interannual to decadal timescales, endogenous changes in forest NEE can arise from disturbance and recovery  
63 (Nelson et al., 1994; Moorcroft et al., 2001; Chambers et al., 2013; Espírito-Santo et al., 2014; Anderegg et al., 2015). The km<sup>67</sup>  
64 eddy flux site in the Tapajós National Forest (TNF) presents a unique opportunity to study the potential legacy of disturbance  
65 caused by drought. This Eastern Brazilian Amazon forest lies on the dry end of the rainfall spectrum for tropical evergreen  
66 forests (Saleska et al., 2003; Hutyra et al., 2005). A severe El Niño drought in 1997-1998 was followed by disturbance,  
67 evidenced by a large and heavily respiring CWD pool in 2001. Subsequent NEE measurements showed a 4-year transition from a  
68 net carbon source in 2002 to nearly carbon-neutral in 2004 and 2005 (Hutyra et al., 2007). The observed disequilibrium state led  
69 researchers to the hypothesis that RE was high but dissipating, and that the forest will continue to transition into equilibrium,  
70 becoming a sink throughout the decade (Pyle et al., 2008). Conversely, this hypothesis implies that any new disturbance should  
71 drive the forest back into disequilibrium, becoming a source again. We test these predictions using meteorological records, forest  
72 inventories of aboveground biomass (AGB) and CWD, and an additional 3.5 years of eddy flux data, resumed after a 2.5-year  
73 interruption, collected since prior studies.

74 In this study, we test hypotheses related to controls of NEE on multiple timescales at an Eastern Amazon rain forest.  
75 Specifically, we sought to answer the following questions: (1) what were the effects of exogenous meteorology upon NEE across  
76 hourly to yearly timescales? (2) What is the seasonal effect of canopy phenology upon NEE? Is phenology synchronized with  
77 wet/dry seasonality? (3) Major basin-wide droughts occurred in 1998 before eddy flux measurements began, and were reported  
78 again in 2005 and 2010 (Zeng et al., 2008; Philips et al., 2009; Lewis et al., 2011; Doughty et al., 2015) during the span of  
79 measurements. Did any of these basin-wide droughts affect the TNF in particular? What was the impact of drought upon  
80 interannual variability and the decadal trend in NEE? Furthermore, which NEE component, GEP or RE, was perturbed most by

81 drought? Overall, we statistically partitioned the multiple influences on NEE across timescales from hours to an entire decade of  
82 eddy flux and forest inventory measurements.

## 83 **2 Methods**

### 84 **2.1 Site Description**

85 The Tapajós National Forest (TNF) is located to the southeast of the convergence of the Tapajós and Amazon Rivers in  
86 Pará, Brazil. The forest site is on the dry end of the spectrum of evergreen tropical forests, receiving 1918 mm of annual rainfall  
87 and experiencing a 5 month long dry season from July 15 to December 14, defined by average monthly precipitation of less than  
88 100 mm (Hutyra et al., 2007). Temperature and humidity average 25 °C and 85% respectively (Rice et al., 2004). The forest has  
89 a closed canopy with a height of roughly 40 m (Stark et al., 2012), emergent trees up to 55 m (Rice et al., 2004). The forest has  
90 fast turnover rates with much of the population consisting of small-diameter trees (Pyle et al., 2008), but many larger trunks, an  
91 uneven age distribution, many epiphytes, and emergent trees; the forest may be considered primary or “old growth” (Goulden et  
92 al., 2004). Soils are predominantly nutrient-poor clay oxisols with some sandy utisols (Rice et al., 2004), both of which have low  
93 organic content and cation exchange capacity. The forest terrain is 75 m upland on a plateau adjacent to the nearby Tapajós  
94 River, and a deep water table accessed by roots sometimes more than 12 meters deep (Hutyra et al., 2007). The flux tower that  
95 provided flux and meteorological data is located near km 67 of the Santarém-Cuiabá highway. The tower and site are designated  
96 by site ID “BR-Sa1” in the FLUXNET data system, but are herein referred to simply as “km67”.

### 97 **2.2 Eddy Covariance Measurements**

98 Hourly fluxes of NEE were calculated using the sum of hourly turbulent eddy fluxes plus the hourly change in height-  
99 weighted average CO<sub>2</sub> concentration in the canopy air column. Our measurements covered two contiguous periods: one from  
100 January 2002 to January 2006 (period 1) and another from July 2008 to December 2011 (period 2). The tower fell in January  
101 2006 when a tree snapped a supporting guy-wire. Measurements resumed in July of 2008 when the tower was rebuilt and  
102 equipment repaired. Measurements ceased again in 2012 when electrical failures damaged measurement and calibration systems.  
103 Some data collection has resumed since 2015, although gaps in this data were much larger than those in periods 1 and 2,  
104 precluding calculating annual carbon balance after 2011.

### 105 **2.3 Flux Data Processing, Quality Control, and Gap Filling**

106 Nighttime NEE measurements were filtered for low turbulence. We used a turbulence threshold filter of  $u_*^{Th} = 0.22$  to  
107 ensure consistency with previous studies (Saleska et al., 2003; Hutyra et al., 2008). The absolute magnitude of nighttime  
108 respiration and resulting carbon balance was highly sensitive to the selection of  $u_*^{Th}$ , (Saleska et al., 2003; Miller et al., 2004).  
109 However, the interannual variability and trend remained the same regardless of the choice of  $u_*^{Th}$  (Saleska et al., 2003). Errors in  
110 total annual NEE therefore do not reflect potentially large  $u_*^{Th}$  error, and should be interpreted as errors in the differences  
111 between years, not errors in the annual magnitude of the carbon source/sink. Coverage of hourly NEE was substantial for both  
112 periods in the total eddy covariance record. After quality control and outlier detection, period 1 (2002-2006) had 80% and period  
113 2 (mid 2008-2011) had 75% data coverage for all hours. Filtering for  $u_*$  below the threshold of 0.22 m/s left 48% and 42%  
114 coverage of period 1 and 2 respectively.

115 We used established gap-filling models to obtain annual NEE totals. Gross ecosystem productivity (GEP) was gap-filled  
116 using a hyperbolic fit curve between GEP and PAR (Waring et al., 1995). For ecosystem respiration (RE), we adapted the  
117 method by Hutrya et al. (2007), who calculated missing, filtered, and daytime hours using 50  $u^*$ -filtered nighttime hour bins,  
118 instead using a running average of 50  $u^*$ -filtered nighttime hours, allowing us to capture the onset of semiannual seasonal  
119 transitions in RE. Consistent with other tropical forest sites, temperature was not used in our gap-filling, because temperature  
120 variability at tropical forests is low, which results in weak and insignificant correlations with RE (Carswell et al., 2002). We  
121 calculated annual errors as 95% bootstrap confidence intervals by resampling like-hours with replacement (NEE conditions for  
122 the same month, time of day, and similar PAR conditions), instead of resampling all hourly NEE, so that resampling did not  
123 capture diurnal and long-term nonstationary.

## 124 **2.4 Meteorological Measurements**

125 Meteorological variables measured at km67 included photosynthetically active radiation (PAR), temperature, and  
126 specific humidity. Downward drifts in PAR data due to a degrading sensor were corrected by de-trending a time series of mid-  
127 day PAR observations in the top 95th percentile of each month (Longo, 2014). This threshold included substantial information  
128 about the sunniest hours, throughout which intensity should remain constant between years for any given month. We scaled the  
129 radiation time series using the proportion between the fitted trend and the initial fitted value. Simultaneous total incoming  
130 shortwave radiation measurements allowed us to partially fill missing periods of PAR data using a relationship derived from  
131 linear regression in simultaneously measured hours ( $R^2 = 0.98$ ).

132 Rainfall measurements were greatly underestimated at this site because of a faulty tipping bucket rain gauge. We  
133 discarded site-based data and calculated a distance-weighted synthetic hourly rainfall time series from a network of nearby  
134 meteorological stations, with locations ranging from 10 km to 110 km away from km67. More information on the meteorological  
135 network is available in Fitzjarrald et al. (2008). Detailed information about the subsequent calculations of the synthetic  
136 precipitation data set and PAR drift correction are available in Longo (2014).

137 Additionally, the Brazil National Institute of Meteorology (INMET) has a station at Belterra, located 25 km away from  
138 km67, with daily precipitation totals dating back to 1971, which were used to corroborate the seasonal and long-term trends at  
139 km67. Correlation between these two monthly datasets for the years 2001-2012 was  $R^2=0.88$ . Altogether there were three data  
140 sets: the local tower-based meteorology, the mesoscale network meteorology data interpolated to km67, and the INMET  
141 meteorology. Further information regarding the robustness of these three datasets, and correlations amongst them, can be found  
142 in Longo (2014). The three datasets provided us with at least two redundant estimates for all meteorological variables at km67.

## 143 **2.5 Coarse Woody Debris and Mortality**

144 To assess how disturbance coincided with changes in NEE, we conducted surveys of coarse woody debris (CWD).  
145 These surveys capture the magnitude and dynamics of the respiring pool of dead tree biomass. Transect subplots were surveyed  
146 in 2001 for pieces greater than 10 cm in diameter (Rice et al., 2004). Bootstrapped confidence intervals were quantified by  
147 resampling subplots totals ( $n=321$ ) with replacement. Additionally, in 2006, pieces only greater than 30 cm in diameter were  
148 surveyed. Lastly, we conducted an additional CWD survey in 2012 using the line-intercept method (Van Wagner, 1968)  
149 throughout all transects for a total length of 4 km to minimize sampling uncertainty. Bootstrap confidence intervals were  
150 quantified by resampling line segment totals ( $n=40$ ) with replacement. These two different methodologies have previously

151 produced consistent simultaneous results within measurement uncertainties, which were 20% larger for line-intercept sampling  
152 than plot-based sampling (Rice et al., 2004).

153 Because CWD surveys were conducted infrequently, we inferred mortality from aboveground biometry surveys in  
154 1999, 2001, 2005, 2008, 2009, 2010, and 2011. Trees larger than 10 cm diameter at breast height (DBH) were surveyed and were  
155 converted to biomass using non-species specific equations (Chambers et al., 2001a) based on sampling previously established  
156 protocols for this site (Rice et al., 2004; Pyle et al., 2008). Mortality biomass was inferred by tallying biomass of dead trees that  
157 were alive in the prior survey. Sometimes, trees were missed by the census surveyors before they could be confirmed dead or  
158 were found again. In 2012 we assigned missing trees that were not later found alive an equal probability of dying in all surveyed  
159 years they had been missing (Longo, 2014). We used tree mortality to model CWD over time using a simple box model with a  
160 first-order rate equation:

$$161 \quad \frac{dCWD}{dt} = -k \cdot CWD + M \quad (1)$$

162 where  $M$  is the mortality rate input to the CWD pool ( $\text{MgC ha}^{-1}\text{yr}^{-1}$ ) and  $k$  is the decay loss rate of  $0.124 \text{ yr}^{-1}$ . The loss rate is  
163 derived from measurements of respiring CWD in Manaus, Amazonas (Chambers et al, 2001b) and snag density measurements  
164 taken at km67 (Rice et al., 2004). The box model initial condition was the 2001 survey of total CWD. This model allowed us to  
165 assess whether disturbances after 2001 were sufficient to cause an increase in CWD or whether disturbances after 2001 were  
166 minimal and the CWD pool respired and depleted gradually. The final timestep of the model was validated against the second  
167 and final full measurement of CWD made in 2012.

## 168 2.6 Empirical NEE Model

169 Our low-parameter empirical model represents the mean response of NEE to hourly and seasonal changes in exogenous  
170 meteorology and seasonal changes in phenology throughout the decade. We used our model to diagnose interannual  
171 nonstationarity in model residuals, which correspond to endogenous ecosystem changes in photosynthesis and respiration rates  
172 between years, give or take random measurement error and unaccounted for model terms. We fit the model to the entire 7.5-year  
173 interrupted eddy covariance record of raw,  $u^*$ -filtered hourly NEE ( $NEE_{\text{obs}}$ ):

$$174 \quad NEE_{\text{Model}} = a_0 + a_1 s_R + \frac{a_2 \text{PAR}}{a_3 + \text{PAR}} \cdot (1 - k_{\text{pheno}} s_{\text{pheno}}) \quad (2)$$

175 where  $NEE_{\text{Model}}$  is the modeled hourly NEE. The models were fit in two steps: first, the two model parameters that represent RE,  
176  $a_0$  and  $a_1$ , were fit to nighttime data, then the remaining three GEP parameters were fit to daytime data. Parameter  $a_0$  is the wet  
177 season intercept for RE. Parameter  $a_1$  is an adjustment of the ecosystem respiration during the rainfall-defined dry season (factor  
178 variable  $s_R$ , defined in detail below). Parameters  $a_2$  and  $a_3$  are the Michaelis-Menten light response parameters. We also include a  
179 simple scaling factor for endogenous changes in phenology: a time-varying binary factor variable  $s_{\text{pheno}}$  represents timing in  
180 changes to the intrinsic light use efficiency ( $LUE=1-k_{\text{pheno}}$ ) within an average seasonal cycle. The purpose of this simplistic  
181 scaling factor was to determine when the timing of endogenous seasonal shifts in LUE that were not explained by light and  
182 moisture were most pronounced.

183 Atmospheric moisture and diffuse radiation, in addition to radiation, are also known to affect photosynthesis at tropical  
184 sites on short timescales (Kiew et al., 2018), by affecting stomatal closure hence controlling the degree to which photosynthetic  
185 uptake saturates at high PAR. We tested a higher-parameter model based on light and moisture model representing exogenous

186 changes to LUE from Wu et al. (2017) to examine whether these meteorological variables added explanatory power to our model  
187 at monthly and longer timescales. This model adjusts LUE by multiplying terms that account for effects of vapor pressure deficit  
188 (VPD:  $1-k_{VPD}$ ) and cloudiness index (CI:  $1-1-k_{CI}$ ) a statistical proxy for diffuse radiation. To determine whether this model was  
189 parsimonious, we evaluated the Bayesian Information Criteria (BIC) of the data-model mean monthly residuals for the model in  
190 Eq. 2 and the higher-parameter light and moisture model. We found that the higher-parameter model was not parsimonious  
191 because the additional parameters did not improve the goodness of fit at monthly timescales. We explain these results further in  
192 Section 3.4.2 and discuss their implications further in Sections 4.1 and 4.2.

193 This forest site has coincident deficits in rainfall and ecosystem RE during the dry season (Saleska et al., 2003; Goulden  
194 et al., 2004) due to desiccation of dead wood, leaf litter, and other substrates for heterotrophic respiration (Hutyra et al., 2008).  
195 To depict this reduced dry season RE, we set dry season  $s_R=1$  and wet season  $s_R=0$ , fitting  $a_I$  to the mean dry season RE. We  
196 defined the dry season onset as the period during which rainfall is below 50 mm per half-month, consistent with previous  
197 definitions of tropical forest dry season as 100 mm month<sup>-1</sup> (e.g. Saleska et al., 2016). We defined the wet season onset as the  
198 first in a series of 3 or more semi-monthly periods with rainfall greater than 50mm; this definition allows for sporadic dry season  
199 downpour whilst ensuring that there is not more than one dry season per year. Although  $a_I$  does not vary across years, our  
200 meteorologically-defined  $s_R$  permits the duration of the dry season to vary interannually. A longer dry season in a given year  
201 would therefore result in less RE (more net uptake) when  $NEE_{Exo}$  is integrated over that full year.

202 We tested three different seasonal timings for the phenology factor variable: (1)  $s_{pheno}=0$  year-round (no phenology), (2)  
203  $s_{pheno}=1$  during the dry season and  $s_{pheno}=0$  during the wet season, and (3)  $s_{pheno}=1$  during the peak of leaf flush (June 15 to Sept  
204 14) (Hutyra et al., 2007) and  $s_{pheno}=0$  all other times of the year. In scenario 2, the timing of phenology varies interannually, but  
205 in scenarios 1 and 3, modeled phenology does not differ between years and therefore does not influence interannual variability in  
206 modeled GEP or NEE.

207 After subtracting hourly  $NEE_{Model}$  from  $NEE_{obs}$ , the annually integrated residuals reflect changes in the ecosystem's  
208 efficiency irrespective of the aggregate response to meteorology, plus or minus random error and unaccounted for meteorological  
209 controls. Upper-level soil moisture, for instance, exerts seasonal controls upon NEE at various tropical sites differently  
210 depending on terrain (Hayek et al., 2018; Kiew et al., 2018) but is not included in the model because it was insignificantly  
211 associated with GEP (Wu et al., 2017) or RE at this site after we controlled for other variables, including wet and dry season  
212 onset, in our model. Examples of a change in intrinsic ecosystem efficiency may occur in the aftermath of a drought, during  
213 which leaf stomates close, causing the ecosystem to sequester less CO<sub>2</sub> per unit incident PAR than average, or a storm inducing  
214 widespread mortality and a pulse of CWD during which RE would be higher than average for a given season or year. In both  
215 scenarios, we would expect residuals to be positive during or after the event, because the ecosystem would sequester less and  
216 emit more CO<sub>2</sub> relative to other years. To assess which aggregated annual residuals were significantly different from zero, we  
217 quantified 95% confidence intervals in annual NEE residuals due to random error using bootstrapping (Section 2.3).

218 We partitioned both  $NEE_{obs}$  and  $NEE_{Model}$  into RE and GEE (GEE = -GEP, to keep the same sign convention as eddy  
219 flux NEE) to determine which of the two components were more adequately represented by our model. For observations of NEE,  
220 RE, and GEE, we used hours during which a direct  $u^*$  filtered measurement of NEE occurred. Observations of RE were  
221 nighttime hours during which NEE was measured; observations of GEE are daytime hours during which the 50-hour running  
222 average RE was subtracted from measured NEE. Partitioned GEE is not a direct observation, but represents the lowest-parameter  
223 approximation of a direct measurement (GEE = NEE - RE see Wu et al., 2017). Our GEE/RE results are limited by not  
224 accounting for partitioning bias.

## 225 **3 Results**

### 226 **3.1 Eddy Covariance Measurements of CO<sub>2</sub> Fluxes**

227 NEE has a large diurnal cycle relative to its mean seasonal cycle, with a mean diel range of 25.05  $\mu\text{mol m}^{-2} \text{s}^{-1}$ . The  
228 range of the mean seasonal cycle is 2.46  $\mu\text{mol m}^{-2} \text{s}^{-1}$ , or 10% of the mean diel range. Annual totals of NEE are presented in Fig.  
229 1. For period 1, the first four years, annual NEE is similar to that reported previously by Hutyra et al. (2007) despite using  
230 slightly modified gap-filling procedures here (Section 2.3). The previously reported trend remains: a moderate source in 2002 of  
231 2.7  $\text{MgC ha}^{-1} \text{yr}^{-1}$  ( $\pm 0.5$  95% bootstrap confidence intervals) tapering off to nearly carbon neutral totals in the following years,  
232 within confidence limits, of 0.5 ( $\pm 0.6$ )  $\text{MgC ha}^{-1} \text{yr}^{-1}$  in 2004 and 0.2 ( $\pm 0.6$ )  $\text{MgC ha}^{-1} \text{yr}^{-1}$  in 2005. During the three subsequent  
233 years that comprise period 2, 2009-2011, the forest returned to a moderate source of carbon, with a range of  $1.8 \pm 0.6 \text{ MgC ha}^{-1}$   
234  $\text{yr}^{-1}$  in 2010 to  $2.5 \pm 0.5 \text{ MgC ha}^{-1} \text{yr}^{-1}$  in 2009. We examined measurements of rainfall, coarse woody debris (CWD), and  
235 aboveground biomass (AGB) for indications of drought or other disturbance during 2002-2011 to explain these patterns seen in  
236 annual NEE totals.

### 237 **3.2 Meteorological Measurements and Drought**

238 We examined our distance-weighted interpolated estimate of km67 rainfall for trends and droughts. Our precipitation  
239 estimate was consistent with previous estimates of precipitation for this site and region, with a minimum of 1595 mm in 2005  
240 and maximum of 2137 mm in 2011 (Saleska et al., 2003; Nepstad et al., 2007). While 2005 annual precipitation was a minimum,  
241 no previous groundwater deficits in carbon exchange, latent heat flux, or sensible heat fluxes were observed during this year  
242 (Hutyra et al, 2007). Our measurements did not indicate that any drought occurred during or immediately preceding period 2 of  
243 NEE measurements. In fact, period 2 annual rainfall totals increased on average by 20% relative to period 1. The dry season in  
244 2009 was longer than average, lasting 6 months (Fig. 2a). Mean annual radiation was expectedly anti-correlated with annual  
245 rainfall. Accordingly, period 2 experienced 4% less mean annual PAR than period 1.

246 Our synthetic decade-long rainfall record corresponded closely with the nearby INMET Belterra measurements,  
247 although INMET Belterra had on average 220 mm of rainfall more per year, likely due to differences in circulation and  
248 convection between the km67 forest and Belterra pasture land surface (Fitzjarrald et al., 2008). Annual rainfall totals throughout  
249 the decade of eddy flux measurements 2002-2011 lay well within the historical variability of annual rainfall since 1972, which  
250 experienced a range of 974 to 3057 mm of annual precipitation (Fig. 2b). The second and third lowest annual precipitation totals  
251 occurred during 1997-1998, which were 1391 and 1218 mm respectively, during a major El Niño event, which persisted from  
252 June of 1997 to June of 1998 (Ross et al., 1998) and corresponded with a 9 month long dry season, the longest in the historical  
253 record.

### 254 **3.3 Coarse woody debris and mortality**

255 We examined measurements of CWD over time to assess whether a disturbance might have impacted the period 2  
256 carbon balance. Compared to CWD stocks in 2001 of 48.6 ( $\pm 5.9$ )  $\text{MgC ha}^{-1}$ , CWD stocks in 2012 were significantly lower at  
257 30.5  $\text{MgC ha}^{-1}$  ( $\pm 7.4$ ) (Fig. 3). Errors in the 2012 pool were 25% larger. The larger magnitude of error is consistent with higher  
258 uncertainty for line-intercept sampling relative to area-based sampling at the TNF (Rice et al., 2004). Because CWD  
259 measurements were sparse in time, we included an additional measurement in 2006 of large CWD, with diameter greater than or  
260 equal to 30 cm, totaling  $20.8 \pm 12.8 \text{ MgC ha}^{-1}$ . We compared this measurement with similarly sized CWD from other surveys

261 (Fig. 3). Total large CWD was  $25.7 \pm 11.4 \text{ MgC ha}^{-1}$  in 2001, and  $19.8 \pm 11.9 \text{ MgC ha}^{-1}$  in 2012. Differences in large CWD  
262 between 2001 and 2006 and between 2006 and 2012 are small relative to their uncertainties, but they still show a qualitative  
263 downward trend over time.

264 A box model of CWD (Eq. 2) allowed us to estimate the transient behavior of the CWD pool throughout years in which  
265 it was not directly measured (Fig. 3). The CWD mortality input rates  $M$  were derived from forest inventory surveys. The box  
266 model shows no large spikes from mortality events outweighing the respiration rate, and its derivative is negative throughout  
267 time, predicting a continuously depleting CWD pool. The box model estimate for 2012 CWD is  $26.2 \text{ MgC ha}^{-1}$ , and lies well  
268 within the uncertainty of the concurrent 2012 measurement. We see no evidence via increased CWD that disturbance has  
269 occurred since the start of measurements.

270 Assuming that the large initial CWD pool arose from a past disturbance, hypothetically following the 1997-1998 El  
271 Niño drought, we ran the CWD box model (Eq. 2) backward in time to estimate the magnitude of such a disturbance. We  
272 assumed that the disturbance occurred in 1998 because 1999 and 2000 were not characterized by below-average rainfall. Severe  
273 drought events have been accompanied by increased mortality and canopy turnover rates in intact Amazon forests (Leitold et al.,  
274 2018). Because the CWD measurement was made in July of 2001, we calculated the box model CWD value to the end of the El  
275 Niño drought in June 1998 using the same respiration rate,  $k$ , and the mean mortality,  $M$ , for all surveys, and applied this rate to  
276 the mean and 95% bootstrapped confidence intervals of the 2001 measurement ( $48.6 \pm 5.9 \text{ MgC ha}^{-1}$ ). Our estimate of the CWD  
277 pool immediately following the drought was thus  $63.7 \pm 8.1 \text{ MgC ha}^{-1}$ . Subtracting the 2012 measurement of  $30.2 \pm 7.3 \text{ MgC ha}^{-1}$   
278 from this number, which is our best estimate of equilibrium CWD that may have existed before the 1997-1998 El Niño drought,  
279 we estimate drought-induced mortality to be  $33.5 \pm 15.4 \text{ MgC ha}^{-1}$ , or 12-31% of present AGB.

## 280 **3.4 Empirical NEE Model**

### 281 **3.4.1 Hourly variability in NEE**

282 Optimized parameter values for our model are included in Table 1. Our model predicted 81% of the variance in  
283 observed hourly NEE, and captured 94% of the amplitude of the diurnal cycle. The only hourly independent variable in the  
284 model was PAR; hourly NEE in our model was therefore predominantly driven by changes in sunlight. Modeled hourly  
285 variability frequently captured the difference in magnitude in NEE between high and low uptake events (example time series  
286 shown in Fig. 4).

### 287 **3.4.2 Seasonal variability in NEE**

288 In our best-fitting model parameterization, phenology was asynchronous with the dry season (Table 2). Over the mean  
289 seasonal cycle, removing this seasonal phenology parameterization resulted in positive residual NEE from June 15 to September  
290 14, hence over-predicting uptake during this time (Fig. 5a). Our final model, however, simplistically corrects for this positive  
291 anomaly, adjusting NEE by 16% (Fig. 5b; Table 2). Although this seasonal transition appears to be more gradual over the season,  
292 our simplistic, low-parameter phenology representation was chosen for parsimony. While the seasonal timing of respiration,  $s_R$ ,  
293 varied by meteorological inputs (semi-monthly total rainfall <50 mm), we could not identify a similar seasonal meteorological  
294 trigger for phenology and therefore used set calendar dates.

295 Our model predicted monthly mean NEE well ( $R^2=0.59$  across all months). Hourly changes in PAR integrated over  
296 monthly and seasonal time periods. Therefore, seasonal variability in our model was controlled by precipitation, sunlight, and a  
297 simplistic parametric representation of phenology (Eq. 2; Table 1).

298 Part of the remaining seasonal variability was explained by random measurement error: bootstrap 95% confidence  
299 intervals representing hourly measurement errors in monthly mean NEE had an average range of  $1.07 \mu\text{mol m}^{-2}\text{s}^{-1}$ , 47% of the  
300 mean NEE seasonal cycle's range. The model slightly over-predicted the mean seasonal cycle's magnitude, although well within  
301 the model and measurement interannual variability (Fig. 6). The model attributed the greatest sink to October, because (1)  
302 October rainfall was low enough each year to be classified as part of the dry season, (2) PAR was consistently high due to sunny  
303 conditions after the dry season onset, and (3) the phenology scaling factor ( $1 - k_{pheno} * s_{pheno}$ ) returned to 1 after Sept 14, increasing  
304 the October LUE and pushing the carbon balance further towards a sink.

305 A higher-parameter model with VPD and diffuse radiation from Wu et al. (2017) explained additional variance in  
306 hourly NEE but not in monthly NEE (Table S1). The BIC score for this model (-31.4) was greater than (more negative) than that  
307 from our main model (-35.6; Eq. 2), because it did not improve the goodness of fit but contained additional parameters. The BIC  
308 results imply that VPD and diffuse radiation do not explain significant additional variance relative to our model (Eq. 2) at  
309 monthly and greater timescales.

### 310 3.4.3 Interannual Variability in NEE

311 Hourly changes in PAR and seasonal changes in precipitation integrated annually to determine yearly sums of modeled  
312 NEE. Therefore, interannual variability was controlled by precipitation and sunlight. Phenology did not vary interannually,  
313 therefore it did not affect interannual variability in modeled NEE.

314 We disaggregated the meteorological influence on NEE, represented by our model (Eq. 2), from long-term changes in  
315 forest's ecological efficiency by examining the annually integrated hourly model residuals. In 2002, there were a total of 1.2  
316  $\text{MgC ha}^{-1}\text{yr}^{-1}$  of excess emissions unaccounted for by the modeled mean response to meteorology (Fig. 7a). The correlation  
317 between modeled and measured yearly NEE was low and insignificant ( $R^2 = 0.17$ ;  $p = 0.37$ ) owing to the 2002 anomaly; if 2002  
318 is excluded as an outlier, the correlation is high and significant ( $R^2 = 0.81$ ;  $p = 0.014$ ). All other years were not significantly  
319 different from zero within random measurement error, represented by 95% bootstrap confidence intervals, indicating that these  
320 years are well predicted by meteorological variability, including the relatively higher emission/lower uptake in period 2 (Fig. 1).

321 On average, period 2 saw a 20% increase in annual precipitation relative to period 1. Abbreviated dry season lengths  
322 and lack of radiation from increased cloudiness in period 2 resulted in less modeled net uptake relative to period 1.

323 We partitioned observed and modeled NEE into RE and GEE. Interannual variations in RE were accurately represented  
324 as changes in wet and dry season length (Fig. S1). The range in annual residual RE is therefore small compared to that of annual  
325 residual GEE (Fig. 7b). In 2002, mean model GEE had  $0.85 \mu\text{mol m}^{-2}\text{s}^{-1}$  more uptake than observations. Therefore, the 1.2  $\text{MgC}$   
326  $\text{ha}^{-1}\text{y}^{-1}$  residual emissions in 2002 were more likely due to anomalously low photosynthesis rather than high RE.

## 327 4 Discussion

### 328 4.1 Hourly and Seasonal Changes in NEE and Implications for Modeling Phenology

329 Hourly changes in NEE were due predominantly to changes in sunlight (Fig. 4). Phenology only played a small role in  
330 modeled hourly variability, improving the fit of our model by only 1% relative to a model that only used meteorology and lacked  
331 a phenology parameterization (Table 2).

332 Seasonal changes, on the other hand, were due to a combination of sunlight, rainfall inputs, and phenology (Fig. 6). The  
333 model parameterization contained a seasonal decrease in respiration ( $a_r$ ) that was synchronous with the dry season, a timing that

334 was consistent with other tropical forest sites, but can exert the opposite influence depending on terrain, drainage, and inundation  
335 (Kiew et al., 2018). A phenological LUE decrease in GEP ( $1-k_{pheno}$ ) was asynchronous with the dry season (Eq. 5; Table 2).  
336 Modeled phenology explained 26% of the variability in observed monthly NEE (Table 2).

337 VPD and diffuse radiation do not explain significant additional variance in NEE relative to our model (Eq. 2) at  
338 monthly timescales (Table 1; Table S1). The relative importance of phenology at monthly timescales, compared to that of VPD  
339 and diffuse radiation, is consistent with other findings regarding GEP at our research site: moving from finer to coarser temporal  
340 resolution, the influence of exogenous meteorology becomes outweighed by that of exogenous ecosystem changes such as those  
341 in phenology (Wu et al. 2017).

342 Seasonal changes in LUE are well explained by canopy leaf age and demography both at this site and at a comparatively  
343 wetter forest site in Manaus, showing good agreement with a model informed by camera and trap-based observations of leaf  
344 flushing and shedding (Wu et al., 2016). Our single mid-year parameter simplistically up-shifts the trough in a more continuous  
345 seasonal oscillation between low and high LUE (Fig. 5) because we lacked independent variables explaining the seasonal  
346 oscillation.

347 The seasonally asynchronous nature of phenology-mediated LUE establishes a middle ground in debates over whether  
348 the Eastern Amazon canopy is enhanced or “greens up” during the dry season (Huete et al., 2006; Myneni et al., 2007; Samanta et  
349 al., 2012; Morton et al., 2014; Bi et al., 2015; Guan et al., 2015; Saleska et al., 2016). Changes to the canopy’s LUE do indeed  
350 occur, but not synchronously with the dry season at our site (Fig. 5). Evidence from previous studies at the TNF suggests that  
351 changes in phenological LUE result from carbon allocation shifting from stem allocation to the turnover and production of new  
352 leaves (Goulden et al., 2004) supporting the prevailing hypothesis that tropical trees have been selected to coordinate new leaf  
353 production ahead of dry seasonal peaks of irradiance (Wright and van Schaik, 1994). The GEP seasonal cycles at additional  
354 evergreen Amazon forest sites are not well described by sunlight alone (Restrepo-Coupe et al., 2013). Averaging over seasonal  
355 windows is therefore likely to miss a potential inter-seasonal depletion and enhancement of canopy LUE if additional regions of  
356 evergreen Amazon forest similarly exhibit seasonally asynchronous phenology.

357 Interannual variation in phenology is represented mechanistically in phenology and LUE sub-models, which have been  
358 optimized using km67 eddy flux data, but nonetheless fail to reproduce the observed mid-year GEP decrease at this site. Kim et  
359 al. (2012) present a light-triggered phenology scheme, which assumes higher modeled leaf turnover rates and higher maximum  
360 leaf photosynthesis during the dry season, and hence produced higher dry season GEP. Their model produced leaf flushing rates  
361 that lagged behind observations, and contradicted observations that light-controlled GEP decreases mid-year at km67 (Fig. 5).  
362 Another phenology scheme has been developed by De Weirdt et al. (2012), which attributes excess leaf allocation to the turnover  
363 of new, more efficient leaves, but nevertheless over-predicted mid-year GEP at km67 relative to their prior model. Wu et al.  
364 (2016), on the other hand, successfully represent the GEP seasonal cycle using their model of leaf age and demography, but  
365 relied on observations of canopy leaf fluxes. Their model, however, does not provide a meteorologically-triggered mechanism  
366 for seasonal leaf shedding and flushing. Therefore, until such a trigger can be identified, models that mechanistically represent  
367 phenology are primed to make erroneous predictions about the interannual and long-term consequences of changing seasonal  
368 lengths for the Amazon carbon balance.

#### 369 **4.2 Interannual variability in NEE**

370 Annual totals of measured NEE exhibited an unpredicted trend: despite previous hypotheses that the years after period 1  
371 would continue to trend downward towards more uptake (Hutyra et al., 2007; Pyle et al., 2008), the ecosystem returned to a  
372 moderate carbon source in all three years of period 2 (Fig. 1). We examined whether the reversal of the period 1 trend throughout

373 period 2 could be explained by exogenous changes in climate or an endogenous biophysical change. We developed the model  
374 selection framework to partition these two sources of variability.

375 Our model represented NEE well across a variety of timescales (Figs. 4, 5, 7). On yearly timescales, interannual  
376 differences in  $NEE_{Model}$  were due to exogenous meteorology, as phenology did not vary interannually. The model predicted  
377 annual NEE accurately within 95% confidence limits of random measurement error for 6 out of 7 years (Fig. 7a), including  
378 period 2, during which the forest returned to a carbon source (Fig. 1). The model representation of the period 2 source was due to  
379 lower radiation and higher rainfall relative to period 1, consistent with findings of light-limitation in Amazon forests derived  
380 from satellite observations of climate and vegetation activity (Nemani et al., 2003).

381 The overall magnitude of the carbon source/sink, however, was highly sensitive to the choice of  $u_*$  filter, consistent with  
382 previous findings (Saleska et al., 2003; Miller et al., 2004; Hayek et al., 2018). We therefore applied a novel correction to the  
383 long-term magnitude of NEE that is independent of the  $u_*$  filter (Hayek et al., 2018), which indicated that the ecosystem may in  
384 fact be a slight sink, but that the interannual variability, which our model represents, remained the same (Fig. S2). The overall  
385 magnitude of the carbon source/sink therefore does not affect or results concerning the variability between years. The least net  
386 uptake still occurred in 2002, from which NEE remained insignificantly different in 2009 and 2011.

387 We examined the possibility that a systematic high bias in 2002 PAR could result in an over-prediction of 2002 GEP  
388 and erroneously cause a positive 2002 residual. We found that PAR was appropriately drift-corrected by corroboration with  $R_{net}$ ,  
389 which was not affected by drifts. Additionally, we note that rainfall was not atypical in 2002 relative to 2003-2005 (Fig. 2).

390 Additional meteorological variables such as the vapor pressure deficit (VPD) and diffuse radiation did not appear to  
391 explain residual NEE in 2002. A model including these variables did not explain the positive NEE/GEE anomaly in 2002 (Fig.  
392 S3). The annual means of both VPD and CI in 2002 lied within their decadal range, making high VPD or low diffuse radiation  
393 unlikely explanations for low photosynthetic uptake. These meteorological factors did not appear to significantly impact  
394 interannual changes in NEE, consistent with previous findings regarding GEP at this site (Wu et al., 2017).

395 We cannot rule out that the 2002 source may be a measurement artifact, caused for example by disturbance following  
396 tower construction. We note, however, that tower construction was completed almost a year before the measurements we used,  
397 with preliminary data collection occurring during 2001 (Saleska et al., 2003). We examine the possibility that 1998 drought-  
398 based disturbance impacted forest GEP through 2002 in section 4.2.2.

#### 399 **4.2.1 Temporal and spatial heterogeneity of droughts**

400 Our multiple records of meteorology adjacent to our research site (Fig. 2), which we used to inform our simple model of  
401 NEE, can also shed light on the larger discussion of recent droughts in the Amazon. Previous reports of 21<sup>st</sup> century droughts in  
402 this region are inconsistent. For the 2010 Amazon drought, Lewis et al. (2011) show that water deficits during were minimal in  
403 the Eastern Amazon region, consistent with our findings. However, Doughty et al. (2015) report ubiquitous detrimental effects of  
404 the 2010 drought basin-wide, including a  $-3 \text{ MgC ha}^{-1}$  GEP anomaly overlying the TNF. Our results contradict these findings: we  
405 did not find anomalously low water inputs, nor a concurrent GEP or NEE anomaly (Fig. 7b), in 2010. For the 2005 Amazon  
406 drought, Zeng et al. (2008) claim that North Tropical Atlantic warming in the dry Jul-Oct quarter led to rainfall reductions  
407 everywhere in the Amazon, a result not borne out by our precipitation analysis. The two supposedly basin-wide droughts in 2005  
408 and 2010 did not appear to affect the region in which this particular site lies. Measurements and empirical modeling of CWD  
409 over time support this finding because no interim disturbances were detected between 2001 and 2011 (Fig. 3). The spatial extent  
410 and severity with which a more recent 2015-2016 El Niño drought impacted Amazon forests, however, remains to be quantified.

## 411 4.2.2 Legacy impacts of drought on ecosystem function

412 Our model over-predicted photosynthetic uptake in 2002, but predicted RE well (Fig. 7b; Fig. S1), suggesting that a  
413 drought-disturbance in 1998 persistently affected forest GEP, not RE, through 2002. These findings contradict a previously  
414 established hypothesis that legacy effects of a prior drought disturbance increased RE in 2002 via increased CWD respiration  
415 ( $R_{\text{CWD}}$ ) and related pathways of decomposition (Saleska et al., 2003; Rice et al, 2004; Hutrya et al., 2007; Pyle et al., 2008).

416 CWD measurements from the km67 site suggest that there was major disturbance before measurements of  $\text{CO}_2$  eddy  
417 fluxes began. Three years after the 1998 drought, there was a large pool of CWD ( $48.6 \text{ MgC ha}^{-1}$  in 2001), implying that a  
418 drought-based disturbance had occurred in the past. By 2012, the CWD pool respired faster than it could accrue additional  
419 necromass from mortality (Fig. 3), implying that no additional impactful disturbance occurred at this site between 2002 and  
420 2012. Although  $R_{\text{CWD}}$  was in fact higher in 2002 than 2005, this difference accounted for only  $0.2 \mu\text{mol m}^{-2} \text{ s}^{-1}$  (Fig. 3) of  
421 respiration. Changes in  $R_{\text{CWD}}$  therefore explain the small differences in annual RE (Fig. S1), but inadequately account for the full  
422  $1.3 \mu\text{mol m}^{-2} \text{ s}^{-1}$  ( $2.4 \text{ MgC ha}^{-1} \text{ yr}^{-1}$ ) difference in NEE between these years (Fig. 1; Fig. 7).

423 Identifying the cause of the reduced 2002 GEP is beyond the scope of this statistical modeling study. It is possible that  
424 the 1997-1998 El Niño drought not only killed entire trees, but also damaged living trees through hydraulic failure and partial  
425 limb death, affecting canopy photosynthesis for subsequent years. An analysis of over 1000 temperate forest census sites  
426 suggests that recovery of live tree biomass accumulation may be delayed by up to four years after drought (Anderegg et al.,  
427 2015). Following the 2005 and 2010 western droughts, findings from forest inventories (Brienen et al., 2015) and remote sensing  
428 (Saatchi et al., 2013), suggested that legacy effects from tropical forest droughts can also persist for four years or more. Drought  
429 cavitation due to xylem embolisms reduces hydraulic conductivity leading to whole tree mortality (Choat et al., 2012), initiating  
430 a classic disturbance-recovery scenario in which felled trees generate canopy gaps for early successional seedlings and saplings  
431 to immediately capitalize on newly available light, causing  $\text{CO}_2$  sources to approximately balance sinks (Chambers et al., 2004).  
432 However, cavitation is also known to cause branch dieback in still living trees (Koch et al., 2004), reducing canopy foliage  
433 partially but not completely forfeiting light resources to the understory. Drought-induced limb diebacks therefore potentially  
434 prolong forest recovery relative to immediate disturbances such as windfall. We hypothesize that partial drought damage to  
435 surviving trees can persistently affect whole-forest photosynthesis. Our findings, that a 1997-1998 drought-disturbance was  
436 followed by reduced photosynthesis in 2002, emphasize the need to better mechanistically understand multi-year legacy impacts  
437 following droughts in evergreen Amazon forests.

## 438 5 Conclusions

439 The decade-long record of eddy flux at km67 in the TNF demonstrated unpredicted trends in 7.5 years of measured  
440 NEE. Our simple, low-parameter empirical model could represent interannual differences in NEE as integrated continuous  
441 responses to changes in meteorology, with exception to the first year, suggesting that increased moisture and decreased sunlight,  
442 not an interim disturbance, were responsible for the elevated period 2 carbon source. Although overall magnitude of the carbon  
443 source/sink was highly sensitive to the specific choice of  $u^*$  filter, the interannual variability, which was predicted by the model,  
444 remained the same. Contrary to some reports, no major drought was apparent in concurrent rainfall records, nor was a major  
445 concurrent disturbance apparent in biometry surveys of this site from 2001 through 2011.

446 Our model represented a seasonal mid-year decline in GEP. Our representation of phenology follows set calendar dates,  
447 and cannot distinguish between various hypotheses concerning the environmental trigger for seasonal leaf shedding and flushing.

448 DVGMs and other numerical simulation ecosystem models that represent phenology as a response to light-triggered leaf flushing  
449 or root water constraints do not tend to represent the seasonal cycle of GEP accurately and are therefore in danger of over-  
450 predicting the future response of photosynthesis to longer dry seasons resulting from climate change.

451 Our finding that reduced photosynthesis, not increased respiration, contributed to the high NEE source in 2002 modifies  
452 the previous hypothesis that the 1997-1998 El Niño drought disturbance affected NEE via respiration. Our findings support a  
453 corollary hypothesis that partial drought-induced damage to still-living trees can impact whole-ecosystem photosynthesis  
454 adversely for multiple years, which is consistent with findings from regional and global-scale forest biometric studies (Anderegg  
455 et al., 2015; Brienen et al., 2015). In order to understand how drought-disturbance uniquely impacts forest recovery,  
456 observational studies and plot-based manipulation experiments are needed in conjunction with models. Such future research is  
457 needed to determine the return times for droughts at which persistent forest biomass loss and collapse may occur.

## 458 **Acknowledgments and Data**

459 This work was supported by funding from a National Science Foundation PIRE fellowship (OISE 0730305) and a U.S.  
460 Department of Energy grant (DE-SC0008311). The eddy flux data used in this study are available online via the Lawrence  
461 Berkeley Laboratories (LBL) Ameriflux network database at <http://ameriflux.lbl.gov/sites/siteinfo/BR-Sa1>.

## 462 **References**

- 463 de Almeida Castanho, A. D., Galbraith, D., Zhang, K., Coe, M. T., Costa, M. H. and Moorcroft, P.: Changing Amazon biomass  
464 and the role of atmospheric CO<sub>2</sub> concentration, climate, and land use, *Global Biogeochem. Cycles*, 30(1), 18–39,  
465 doi:10.1002/2015GB005135, 2016.
- 466 Anderegg, W. R. L., Schwalm, C., Biondi, F., Camarero, J. J., Koch, G., Litvak, M., Ogle, K., Shaw, J. D., Shevliakova, E.,  
467 Williams, A. P., Wolf, A., Ziaco, E. and Pacala, S.: Pervasive drought legacies in forest ecosystems and their  
468 implications for carbon cycle models, *Science* (80-. ), 349(6247), 528–532, doi:10.1126/science.aab1833, 2015.
- 469 Baldocchi, D. D.: Assessing the eddy covariance technique for evaluating carbon dioxide exchange rates of ecosystems: Past,  
470 present and future, *Glob. Chang. Biol.*, 9(4), 479–492, doi:10.1046/j.1365-2486.2003.00629.x, 2003.
- 471 Barford, C. C., Wofsy, S. C., Goulden, M. L., Munger, J. W., Pyle, E. H., Urbanski, S. P., Hutyyra, L., Saleska, S. R., Fitzjarrald,  
472 D. and Moore, K.: Factors Controlling Long- and Short-Term Sequestration of Atmospheric CO<sub>2</sub> in a Mid-latitude  
473 Forest, *Science* (80-. ), 294(5547), 1688–1691, doi:10.1126/science.1062962, 2001.
- 474 Betts, R. a., Cox, P. M., Collins, M., Harris, P. P., Huntingford, C. and Jones, C. D.: The role of ecosystem-atmosphere  
475 interactions in simulated Amazonian precipitation decrease and forest dieback under global climate warming, *Theor.*  
476 *Appl. Climatol.*, 78(1–3), 157–175, doi:10.1007/s00704-004-0050-y, 2004.
- 477 Bi, J., Knyazikhin, Y., Choi, S., Park, T., Barichivich, J., Ciais, P., Fu, R., Ganguly, S., Hall, F., Hilker, T., Huete, A., Jones, M.,  
478 Kimball, J., Lyapustin, A. I., Möttus, M., Nemani, R. R., Piao, S., Poulter, B., Saleska, S. R., Saatchi, S. S., Xu, L.,  
479 Zhou, L. and Myneni, R. B.: Sunlight mediated seasonality in canopy structure and photosynthetic activity of  
480 Amazonian rainforests, *Environ. Res. Lett.*, 10(6), 64014, doi:10.1088/1748-9326/10/6/064014, 2015.
- 481 Bolker, B. M., Pacala, S. W. and Parton, W. J.: Linear analysis of soil decomposition: Insights from the Century model, *Ecol.*  
482 *Appl.*, 8(2), 425–439, doi:10.1890/1051-0761(1998)008[0425:LAOSDI]2.0.CO;2, 1998.
- 483 Brienen, R. J. W., Phillips, O. L., Feldpausch, T. R., Gloor, E., Baker, T. R., Lloyd, J., Lopez-Gonzalez, G., Monteagudo-  
484 Mendoza, A., Malhi, Y., Lewis, S. L., Vásquez Martínez, R., Alexiades, M., Álvarez Dávila, E., Alvarez-Loayza, P.,  
485 Andrade, A., Aragão, L. E. O. C., Araujo-Murakami, A., Arets, E. J. M. M., Arroyo, L., Aymard C, G. A., Bánki, O. S.,  
486 Baraloto, C., Barroso, J., Bonal, D., Boot, R. G. A., Camargo, J. L. C., Castilho, C. V., Chama, V., Chao, K. J., Chave,  
487 J., Comiskey, J. A., Cornejo Valverde, F., da Costa, L., de Oliveira, E. A., Di Fiore, A., Erwin, T. L., Fauset, S.,  
488 Forsthofer, M., Galbraith, D. R., Grahame, E. S., Groot, N., Hérault, B., Higuchi, N., Honorio Coronado, E. N.,  
489 Keeling, H., Killeen, T. J., Laurance, W. F., Laurance, S., Licona, J., Magnussen, W. E., Marimon, B. S., Marimon-  
490 Junior, B. H., Mendoza, C., Neill, D. A., Nogueira, E. M., Núñez, P., Pallqui Camacho, N. C., Parada, A., Pardo-

- 491 Molina, G., Peacock, J., Peña-Claros, M., Pickavance, G. C., Pitman, N. C. A., Poorter, L., Prieto, A., Quesada, C. A.,  
 492 Ramírez, F., Ramírez-Angulo, H., Restrepo, Z., Roopsind, A., Rudas, A., Salomão, R. P., Schwarz, M., Silva, N., Silva-  
 493 Espejo, J. E., Silveira, M., Stropp, J., Talbot, J., ter Steege, H., Teran-Aguilar, J., Terborgh, J., Thomas-Caesar, R.,  
 494 Toledo, M., Torello-Raventos, M., Umetsu, R. K., van der Heijden, G. M. F., van der Hout, P., Guimarães Vieira, I. C.,  
 495 Vieira, S. A., Vilanova, E., Vos, V. A. and Zagt, R. J.: Long-term decline of the Amazon carbon sink., *Nature*,  
 496 519(7543), 344–8, doi:10.1038/nature14283, 2015.
- 497 Carswell, F. E., Costa, a. L., Palheta, M., Malhi, Y., Meir, P., Costa, J. D. P. R., Ruivo, M. D. L., Leal, L. D. S. M., Costa, J. M.  
 498 N., Clement, R. J. and Grace, J.: Seasonality in CO<sub>2</sub> and H<sub>2</sub>O flux at an eastern Amazonian rain forest, *J. Geophys.*  
 499 *Res. D Atmos.*, 107(20), 8076, doi:10.1029/2000JD000284, 2002.
- 500 Chambers, J. Q., Santos, J. Dos, Ribeiro, R. J. and Higuchi, N.: Tree damage, allometric relationships, and above-ground net  
 501 primary production in central Amazon forest, *For. Ecol. Manage.*, 152(1–3), 73–84, doi:10.1016/S0378-  
 502 1127(00)00591-0, 2001a.
- 503 Chambers, J. Q., Schimel, J. P. and Nobre, A. D.: Respiration from coarse wood litter in central Amazon forests,  
 504 *Biogeochemistry*, 52(2), 115–131, doi:10.1023/A:1006473530673, 2001b.
- 505 Chambers, J. Q., Higuchi, N., Teixeira, L. M., dos Santos, J., Laurance, S. G. and Trumbore, S. E.: Response of tree biomass and  
 506 wood litter to disturbance in a Central Amazon forest., *Oecologia*, 141(4), 596–611, doi:10.1007/s00442-004-1676-2,  
 507 2004.
- 508 Chambers, J. Q., Negron-Juarez, R. I., Marra, D. M., Di Vittorio, A., Tews, J., Roberts, D., Ribeiro, G. H. P. M., Trumbore, S. E.  
 509 and Higuchi, N.: The steady-state mosaic of disturbance and succession across an old-growth Central Amazon forest  
 510 landscape, *Proc. Natl. Acad. Sci.*, 110(10), 3949–3954, doi:10.1073/pnas.1202894110, 2013.
- 511 Choat, B., Jansen, S., Brodribb, T. J., Cochard, H., Delzon, S., Bhaskar, R., Bucci, S. J., Feild, T. S., Gleason, S. M., Hacke, U.  
 512 G., Jacobsen, A. L., Lens, F., Maherali, H., Martínez-Vilalta, J., Mayr, S., Mencuccini, M., Mitchell, P. J., Nardini, A.,  
 513 Pittermann, J., Pratt, R. B., Sperry, J. S., Westoby, M., Wright, I. J. and Zanne, A. E.: Global convergence in the  
 514 vulnerability of forests to drought., *Nature*, 491(7426), 752–5, doi:10.1038/nature11688, 2012.
- 515 Collatz, G. J., Ball, J. T., Grivet, C. and Berry, J. A.: Physiological and environmental regulation of stomatal conductance,  
 516 photosynthesis and transpiration: a model that includes a laminar boundary layer, *Agric. For. Meteorol.*, 54(2–4), 107–  
 517 136, doi:10.1016/0168-1923(91)90002-8, 1991.
- 518 De Weirdt, M., Verbeeck, H., Maignan, F., Peylin, P., Poulter, B., Bonal, D., Ciais, P. and Steppe, K.: Seasonal leaf dynamics  
 519 for tropical evergreen forests in a process-based global ecosystem model, *Geosci. Model Dev.*, 5(5), 1091–1108,  
 520 doi:10.5194/gmd-5-1091-2012, 2012.
- 521 Doughty, C. E. and Goulden, M. L.: Seasonal patterns of tropical forest leaf area index and CO<sub>2</sub> exchange, *J. Geophys. Res.*  
 522 *Biogeosciences*, 113(G1), G00B06, doi:10.1029/2007JG000590, 2008.
- 523 Doughty, C. E., Metcalfe, D. B., Girardin, C. A. J., Amézquita, F. F., Cabrera, D. G., Huasco, W. H., Silva-Espejo, J. E., Araujo-  
 524 Murakami, A., da Costa, M. C., Rocha, W., Feldpausch, T. R., Mendoza, A. L. M., da Costa, A. C. L., Meir, P., Phillips,  
 525 O. L. and Malhi, Y.: Drought impact on forest carbon dynamics and fluxes in Amazonia, *Nature*, 519(7541), 78–82,  
 526 doi:10.1038/nature14213, 2015.
- 527 Duffy, P. B., Brando, P., Asner, G. P. and Field, C. B.: Projections of future meteorological drought and wet periods in the  
 528 Amazon, *Proc. Natl. Acad. Sci.*, 112(43), 13172–13177, doi:10.1073/pnas.1421010112, 2015.
- 529 Dunn, A. L., Barford, C. C., Wofsy, S. C., Goulden, M. L. and Daube, B. C.: A long-term record of carbon exchange in a boreal  
 530 black spruce forest: means, responses to interannual variability, and decadal trends, *Glob. Chang. Biol.*, 13(3), 577–590,  
 531 doi:10.1111/j.1365-2486.2006.01221.x, 2007.
- 532 Espírito-Santo, F. D. B. B., Gloor, M., Keller, M., Malhi, Y., Saatchi, S., Nelson, B., Junior, R. C. O., Pereira, C., Lloyd, J.,  
 533 Frolking, S., Palace, M., Shimabukuro, Y. E., Duarte, V., Mendoza, A. M., López-González, G., Baker, T. R.,  
 534 Feldpausch, T. R., Brienen, R. J. W. W., Asner, G. P., Boyd, D. S. and Phillips, O. L.: Size and frequency of natural  
 535 forest disturbances and the Amazon forest carbon balance, *Nat. Commun.*, 5, 1–6, doi:10.1038/ncomms4434, 2014.
- 536 Farrior, C. E., Rodriguez-Iturbe, I., Dybzinski, R., Levin, S. a and Pacala, S. W.: Decreased water limitation under elevated CO<sub>2</sub>  
 537 amplifies potential for forest carbon sinks, *Proc. Natl. Acad. Sci.*, 112(23), 7213–7218, doi:10.1073/pnas.1506262112,  
 538 2015. Fatichi, S., Leuzinger, S. and Körner, C.: Moving beyond photosynthesis: from carbon source to sink-driven  
 539 vegetation modeling, *New Phytol.*, 201(4), 1086–1095, doi:10.1111/nph.12614, 2014.
- 540 Fitzjarrald, D. R., Sakai, R. K., Moraes, O. L. L., De Oliveira, R. C., Acevedo, O. C., Czikowsky, M. J. and Beldini, T.: Spatial  
 541 and temporal rainfall variability near the amazon-tapajós confluence, *J. Geophys. Res. Biogeosciences*, 114(1),  
 542 G00B11, doi:10.1029/2007JG000596, 2008.

- 543 Frey, S. D., Lee, J., Melillo, J. M. and Six, J.: The temperature response of soil microbial efficiency and its feedback to climate,  
544 *Nat. Clim. Chang.*, 3(4), 395–398, doi:10.1038/nclimate1796, 2013.
- 545 Goulden, M. L., Miller, S. D., Da Rocha, H. R., Menton, M. C., De Freitas, H. C., E Silva Figueira, A. M. and Dias De Sousa, C.  
546 A.: Diel and seasonal patterns of tropical forest CO<sub>2</sub> exchange, *Ecol. Appl.*, 14(4 SUPPL.), 42–54, doi:10.1890/02-  
547 6008, 2004.
- 548 Guan, K., Pan, M., Li, H., Wolf, A., Wu, J., Medvigy, D., Caylor, K. K., Sheffield, J., Wood, E. F., Malhi, Y., Liang, M.,  
549 Kimball, J. S., Saleska, S. R., Berry, J., Joiner, J. and Lyapustin, A. I.: Photosynthetic seasonality of global tropical  
550 forests constrained by hydroclimate, *Nat. Geosci.*, 8(4), 284–289, doi:10.1038/ngeo2382, 2015.
- 551 Hayek, M. N., Wehr, R., Longo, M., Hutyra, L. R., Wiedemann, K., Munger, J. W., Bonal, D., Saleska, S. R., Fitzjarrald, D. R.  
552 and Wofsy, S. C.: A novel correction for biases in forest eddy covariance carbon balance, *Agric. For. Meteorol.*, 250–  
553 251(July 2017), 90–101, doi:10.1016/j.agrformet.2017.12.186, 2018.
- 554 Houghton, R. a, Lawrence, K. T., Hackler, J. L. and Brown, S.: The spatial distribution of forest biomass in the Brazilian  
555 Amazon: a comparison of estimates, *Glob. Chang. Biol.*, 7(7), 731–746, doi:DOI 10.1046/j.1365-2486.2001.00426.x,  
556 2001.
- 557 Huete, A. R., Didan, K., Shimabukuro, Y. E., Ratana, P., Saleska, S. R., Hutyra, L. R., Yang, W., Nemani, R. R. and Myneni, R.:  
558 Amazon rainforests green-up with sunlight in dry season, *Geophys. Res. Lett.*, 33(6), 2–5, doi:10.1029/2005GL025583,  
559 2006.
- 560 Hutyra, L. R., Munger, J. W., Nobre, C. a., Saleska, S. R., Vieira, S. a. and Wofsy, S. C.: Climatic variability and vegetation  
561 vulnerability in Amazônia, *Geophys. Res. Lett.*, 32(24), L24712, doi:10.1029/2005GL024981, 2005.
- 562 Hutyra, L. R., Munger, J. W., Saleska, S. R., Gottlieb, E., Daube, B. C., Dunn, A. L., Amaral, D. F., de Camargo, P. B. and  
563 Wofsy, S. C.: Seasonal controls on the exchange of carbon and water in an Amazonian rain forest, *J. Geophys. Res.*  
564 *Biogeosciences*, 112(3), G03008, doi:10.1029/2006JG000365, 2007.
- 565 Hutyra, L. R., Munger, J. W., Hammond-Pyle, E., Saleska, S. R., Restrepo-Coupe, N., Daube, B. C., de Camargo, P. B. and  
566 Wofsy, S. C.: Resolving systematic errors in estimates of net ecosystem exchange of CO<sub>2</sub> and ecosystem respiration in  
567 a tropical forest biome, *Agric. For. Meteorol.*, 148(8–9), 1266–1279, doi:10.1016/j.agrformet.2008.03.007, 2008.
- 568 Kiew, F., Hirata, R., Hirano, T., Wong, G. X., Aeries, E. B., Musin, K. K., Waili, J. W., Lo, K. S., Shimizu, M. and Melling, L.:  
569 CO<sub>2</sub> balance of a secondary tropical peat swamp forest in Sarawak, Malaysia, *Agric. For. Meteorol.*, 248 (October  
570 2017), 494–501, doi:10.1016/j.agrformet.2017.10.022, 2018.
- 571 Kim, Y., Knox, R. G., Longo, M., Medvigy, D., Hutyra, L. R., Pyle, E. H., Wofsy, S. C., Bras, R. L. and Moorcroft, P. R.:  
572 Seasonal carbon dynamics and water fluxes in an Amazon rainforest, *Glob. Chang. Biol.*, 18(4), 1322–1334,  
573 doi:10.1111/j.1365-2486.2011.02629.x, 2012.
- 574 Koch, G. W., Sillett, S. C., Jennings, G. M. and Davis, S. D.: The limits to tree height, *Nature*, 428(6985), 851–854,  
575 doi:10.1038/nature02417, 2004.
- 576 Leitold, V., Morton, D. C., Longo, M., dos-Santos, M. N., Keller, M. and Scaranello, M.: El Niño drought increased canopy  
577 turnover in Amazon forests, *New Phytol.*, 959–971, doi:10.1111/nph.15110, 2018.
- 578 Lewis, S. L., Brando, P. M., Phillips, O. L., van der Heijden, G. M. F. and Nepstad, D.: The 2010 Amazon Drought, *Science* (80-  
579 .), 331(6017), 554–554, doi:10.1126/science.1200807, 2011.
- 580 Longo, M.: Amazon Forest Response to Changes in Rainfall Regime: Results from an Individual-Based Dynamic Vegetation  
581 Model, Doctoral dissertation, Harvard University, 2014.
- 582 Longo, M., Knox, R. G., Levine, N. M., Alves, L. F., Bonal, D., Camargo, P. B., Fitzjarrald, D. R., Hayek, M. N., Restrepo-  
583 Coupe, N., Saleska, S. R., da Silva, R., Stark, S. C., Tapajós, R. P., Wiedemann, K. T., Zhang, K., Wofsy, S. C. and  
584 Moorcroft, P. R.: Ecosystem heterogeneity and diversity mitigate Amazon forest resilience to frequent extreme  
585 droughts, *New Phytol.*, doi:10.1111/nph.15185, 2018.
- 586 McDowell, N., Allen, C. D., Anderson-Teixeira, K., Brando, P., Brien, R., Chambers, J., Christoffersen, B., Davies, S.,  
587 Doughty, C., Duque, A., Espirito-Santo, F., Fisher, R., Fontes, C. G., Galbraith, D., Goodsman, D., Grossiord, C.,  
588 Hartmann, H., Holm, J., Johnson, D. J., Kassim, A. R., Keller, M., Koven, C., Kueppers, L., Kumagai, T., Malhi, Y.,  
589 McMahon, S. M., Mencuccini, M., Meir, P., Moorcroft, P., Muller-Landau, H. C., Phillips, O. L., Powell, T., Sierra, C.  
590 A., Sperry, J., Warren, J., Xu, C. and Xu, X.: Drivers and mechanisms of tree mortality in moist tropical forests, *New*  
591 *Phytol.*, doi:10.1111/nph.15027, 2018.

- 592 Melillo, J. M., Steudler, P. a, Aber, J. D., Newkirk, K., Lux, H., Bowles, F. P., Catricala, C., Magill, a, Ahrens, T. and  
593 Morrisseau, S.: Soil warming and carbon-cycle feedbacks to the climate system., *Science*, 298(5601), 2173–2176,  
594 doi:10.1126/science.1074153, 2002.
- 595 Miller, S. D., Goulden, M. L., Menton, M. C., Da Rocha, H. R., De Freitas, H. C., E Silva Figueira, A. M. and De Sousa, C. A.  
596 D.: Biometric and micrometeorological measurements of tropical forest carbon balance, *Ecol. Appl.*, 14(4 SUPPL.),  
597 114–126, doi:10.1890/02-6005, 2004.
- 598 Moorcroft, P. R., Hurtt, G. C. and Pacala, S. W.: a Method for Scaling Vegetation Dynamics: the Ecosystem Demography Model  
599 (Ed), *Ecol. Monogr.*, 71(4), 557–586, doi:10.1890/0012-9615(2001)071[0557:AMFSVD]2.0.CO;2, 2001.
- 600 Morton, D. C., Defries, R. S., Randerson, J. T., Giglio, L., Schroeder, W. and Van Der Werf, G. R.: Agricultural intensification  
601 increases deforestation fire activity in Amazonia, *Glob. Chang. Biol.*, 14(10), 2262–2275, doi:10.1111/j.1365-  
602 2486.2008.01652.x, 2008.
- 603 Morton, D. C., Rubio, J., Cook, B. D., Gastellu-Etchegorry, J. P., Longo, M., Choi, H., Hunter, M. and Keller, M.: Amazon  
604 forest structure generates diurnal and seasonal variability in light utilization, *Biogeosciences*, 13(7), 2195–2206,  
605 doi:10.5194/bg-13-2195-2016, 2016.
- 606 Myneni, R. B., Yang, W., Nemani, R. R., Huete, A. R., Dickinson, R. E., Knyazikhin, Y., Didan, K., Fu, R., Negrón Juárez, R. I.,  
607 Saatchi, S. S., Hashimoto, H., Ichii, K., Shabanov, N. V., Tan, B., Ratana, P., Privette, J. L., Morisette, J. T., Vermote, E.  
608 F., Roy, D. P., Wolfe, R. E., Friedl, M. a, Running, S. W., Votava, P., El-Saleous, N., Devadiga, S., Su, Y. and  
609 Salomonson, V. V: Large seasonal swings in leaf area of Amazon rainforests., *Proc. Natl. Acad. Sci. U. S. A.*, 104(12),  
610 4820–4823, doi:10.1073/pnas.0611338104, 2007.
- 611 Nelson, B. W., Kapos, V., Adams, J. B., Oliveira, W. J. and Oscar, P. G.: Forest Disturbance by Large Blowdowns in the  
612 Brazilian Amazon, *Ecology*, 75(3), 853–858, 1994.
- 613 Nemani, R. R., Keeling, C. D., Hashimoto, H., Jolly, W. M., Piper, S. C., Tucker, C. J., Myneni, R. B. and Running, S. W.:  
614 Climate-driven increases in global terrestrial net primary production from 1982 to 1999, *Science* (80- ), 300(5625),  
615 1560–1563, doi:10.1126/science.1082750, 2003.
- 616 Nepstad, D. C., Tohver, I. M., Ray, D., Moutinho, P. and Cardinot, G.: Mortality of large trees and lianas following experimental  
617 drought in an Amazon forest., *Ecology*, 88(9), 2259–69, 2007.
- 618 Phillips, O. L., Aragão, L. E. O. C., Lewis, S. L., Fisher, J. B., Lloyd, J., López-gonzález, G., Malhi, Y., Monteagudo, A.,  
619 Peacock, J., Quesada, C. A., Heijden, G. Van Der, Almeida, S., Amaral, I., Arroyo, L., Aymard, G., Baker, T. R., Bánki,  
620 O., Blanc, L., Bonal, D., Brando, P., Chave, J., Cristina, Á., Oliveira, A. De, Cardozo, N. D., Czimczik, C. I.,  
621 Feldpausch, T. R., Freitas, M. A., Gloor, E., Higuchi, N., Jiménez, E., Lloyd, G., Meir, P., Mendoza, C., Morel, A.,  
622 Neill, D. A., Nepstad, D., Patiño, S., Peñuela, M. C., Prieto, A., Ramírez, F., Schwarz, M., Silva, J., Silveira, M.,  
623 Thomas, A. S., Steege, H., Stropp, J., Vásquez, R., Zelazowski, P., Dávila, E. A., Andelman, S., Andrade, A., Chao, K.,  
624 Erwin, T., Fiore, A. Di, C. E. H., Keeling, H., Killeen, T. J., Laurance, W. F., Cruz, A. P., Pitman, N. C. A., Vargas, P.  
625 N., Ramírez-angulo, H., Rudas, A. and Salamão, R.: Drought Sensitivity of the Amazon Rainforest, *Science* (80- ),  
626 323(March), 1344–1347, doi:10.1126/science.1164033, 2009.
- 627 Pyle, E. H., Santoni, G. W., Nascimento, H. E. M., Hutyrá, L. R., Vieira, S., Curran, D. J., van Haren, J., Saleska, S. R., Chow,  
628 V. Y., Carmago, P. B., Laurance, W. F. and Wofsy, S. C.: Dynamics of carbon, biomass, and structure in two  
629 Amazonian forests, *J. Geophys. Res. Biogeosciences*, 113(G1), n/a-n/a, doi:10.1029/2007JG000592, 2008.
- 630 Restrepo-Coupe, N., da Rocha, H. R., Hutyrá, L. R., da Araujo, A. C., Borma, L. S., Christoffersen, B., Cabral, O. M. R., de  
631 Camargo, P. B., Cardoso, F. L., da Costa, A. C. L., Fitzjarrald, D. R., Goulden, M. L., Kruijt, B., Maia, J. M. F., Malhi,  
632 Y. S., Manzi, A. O., Miller, S. D., Nobre, A. D., von Randow, C., Sá, L. D. A., Sakai, R. K., Tota, J., Wofsy, S. C.,  
633 Zanchi, F. B. and Saleska, S. R.: What drives the seasonality of photosynthesis across the Amazon basin? A cross-site  
634 analysis of eddy flux tower measurements from the Brasil flux network, *Agric. For. Meteorol.*, 182–183, 128–144,  
635 doi:10.1016/j.agrformet.2013.04.031, 2013.
- 636 Rice, A. H., Pyle, E. H., Saleska, S. R., Hutyrá, L., Palace, M., Keller, M., de Camargo, P. B., Portilho, K., Marques, D. F. and  
637 Wofsy, S. C.: Carbon Balance and Vegetation Dynamics in an Old-Growth Amazonian Forest, *Ecol. Appl.*, 14(sp4),  
638 55–71, doi:10.1890/02-6006, 2004.
- 639 Ross, T., Lott, N., McCown, S. and Quinn, D.: The El Nino Winter of '97 - '98, NOAA Natl. Clim. Data Cent. Tech. Reports 98-  
640 02, 28, 1998.
- 641 Saatchi, S., Asefi-Najafabady, S., Malhi, Y., Aragao, L. E. O. C., Anderson, L. O., Myneni, R. B. and Nemani, R.: Persistent  
642 effects of a severe drought on Amazonian forest canopy, *Proc. Natl. Acad. Sci.*, 110(2), 565–570,  
643 doi:10.1073/pnas.1204651110, 2013.

- 644 Saleska, S.R., Wu, J., Guan, K., Restrepo-Coupe, N., Nobre, AD., Araujo, A., and Huete, A. R.: Dry-season greening of Amazon  
645 forests., *Nat. Br. Commun. Aris.*, 531(7594), E4–E5, doi:10.1038/nature16457, 2016.
- 646 Saleska, S. R., Miller, S. D., Matross, D. M., Goulden, M. L., Wofsy, S. C., da Rocha, H. R., de Camargo, P. B., Crill, P., Daube,  
647 B. C., de Freitas, H. C., Hutyra, L., Keller, M., Kirchhoff, V., Menton, M., Munger, J. W., Pyle, E. H., Rice, A. H. and  
648 Silva, H.: Carbon in Amazon forests: unexpected seasonal fluxes and disturbance-induced losses., *Science*, 302(5650),  
649 1554–7, doi:10.1126/science.1091165, 2003.
- 650 Samanta, A., Knyazikhin, Y., Xu, L., Dickinson, R. E., Fu, R., Costa, M. H., Saatchi, S. S., Nemani, R. R. and Myneni, R. B.:  
651 Seasonal changes in leaf area of Amazon forests from leaf flushing and abscission, *J. Geophys. Res. Biogeosciences*,  
652 117(1), G01015, doi:10.1029/2011JG001818, 2012.
- 653 Stark, S. C., Leitold, V., Wu, J. L., Hunter, M. O., de Castilho, C. V, Costa, F. R. C., McMahon, S. M., Parker, G. G.,  
654 Shimabukuro, M. T., Lefsky, M. a, Keller, M., Alves, L. F., Schiatti, J., Shimabukuro, Y. E., Brandão, D. O.,  
655 Woodcock, T. K., Higuchi, N., de Camargo, P. B., de Oliveira, R. C., Saleska, S. R. and Chave, J.: Amazon forest  
656 carbon dynamics predicted by profiles of canopy leaf area and light environment., *Ecol. Lett.*, 15(12), 1406–14,  
657 doi:10.1111/j.1461-0248.2012.01864.x, 2012.
- 658 Urbanski, S., Barford, C., Wofsy, S., Kucharik, C., Pyle, E., Budney, J., McKain, K., Fitzjarrald, D., Czikowsky, M. and  
659 Munger, J. W.: Factors controlling CO<sub>2</sub> exchange on timescales from hourly to decadal at Harvard Forest, *J. Geophys.*  
660 *Res. Biogeosciences*, 112(2), G02020, doi:10.1029/2006JG000293, 2007.
- 661 Van Wagner, C. E.: The Line Intersect Method in Forest Fuel Sampling, *For. Sci.*, 14(1), 20–26, 1968. Verbeeck, H., Peylin, P.,  
662 Bacour, C., Bonal, D., Steppe, K. and Ciais, P.: Seasonal patterns of CO<sub>2</sub> fluxes in Amazon forests: Fusion of eddy  
663 covariance data and the ORCHIDEE model, *J. Geophys. Res. Biogeosciences*, 116(G2), G02018,  
664 doi:10.1029/2010JG001544, 2011.
- 665 Waring, R. H., Law, B. E., Goulden, M. L., Bassow, S. L., McCreight, R. W., Wofsy, S. C. and Bazzaz, F. a.: Scaling gross  
666 ecosystem production at Harvard Forest with remote sensing: A comparison of estimates from a constrained quantum-  
667 use efficiency model and eddy correlation, *Plant, Cell Environ.*, 18(10), 1201–1213, doi:10.1111/j.1365-  
668 3040.1995.tb00629.x, 1995.
- 669 Wright, S. J. and van Schaik, C. P.: Light and the Phenology of Tropical Trees, *Am. Nat.*, 143(1), 192, doi:10.1086/285600,  
670 1994.
- 671 Wu, J., Albert, L. P., Lopes, A. P., Restrepo-Coupe, N., Hayek, M., Wiedemann, K. T., Guan, K., Stark, S. C., Christoffersen, B.,  
672 Prohaska, N., Tavares, J. V., Marostica, S., Kobayashi, H., Ferreira, M. L., Campos, K. S., Silva, R. da, Brando, P. M.,  
673 Dye, D. G., Huxman, T. E., Huete, A. R., Nelson, B. W. and Saleska, S. R.: Leaf development and demography explain  
674 photosynthetic seasonality in Amazon evergreen forests, *Science* (80-. ), 351(6276), 972–977,  
675 doi:10.1126/science.aad5068, 2016.
- 676 Wu, J., Guan, K., Hayek, M., Restrepo-Coupe, N., Wiedemann, K. T., Xu, X., Wehr, R., Christoffersen, B. O., Miao, G., da  
677 Silva, R., de Araujo, A. C., Oliviera, R. C., Camargo, P. B., Monson, R. K., Huete, A. R. and Saleska, S. R.:  
678 Partitioning controls on Amazon forest photosynthesis between environmental and biotic factors at hourly to interannual  
679 timescales, *Glob. Chang. Biol.*, 23(3), 1240–1257, doi:10.1111/gcb.13509, 2017.
- 680 Yadav, V., Mueller, K. L., Dragoni, D. and Michalak, A. M.: A geostatistical synthesis study of factors affecting gross primary  
681 productivity in various ecosystems of North America, *Biogeosciences*, 7(9), 2655–2671, doi:10.5194/bg-7-2655-2010,  
682 2010.
- 683 Zeng, N., Yoon, J.-H., Marengo, J. a, Subramaniam, A., Nobre, C. a, Mariotti, A. and Neelin, J. D.: Causes and impacts of the  
684 2005 Amazon drought, *Environ. Res. Lett.*, 3(1), 14002, doi:10.1088/1748-9326/3/1/014002, 2008.
- 685 Zscheischler, J., Mahecha, M. D., Avitabile, V., Calle, L., Carvalhais, N., Ciais, P., Gans, F., Gruber, N., Hartmann, J., Herold,  
686 M., Ichii, K., Jung, M., Landschützer, P., Laruelle, G. G., Lauerwald, R., Papale, D., Peylin, P., Poulter, B., Ray, D.,  
687 Regnier, P., Rödenbeck, C., Roman-Cuesta, R. M., Schwalm, C., Tramontana, G., Tyukavina, A., Valentini, R., van der  
688 Werf, G., West, T. O., Wolf, J. E. and Reichstein, M.: Reviews and syntheses: An empirical spatiotemporal description  
689 of the global surface–atmosphere carbon fluxes: opportunities and data limitations, *Biogeosciences*, 14(15), 3685–3703,  
690 doi:10.5194/bg-14-3685-2017, 2017.

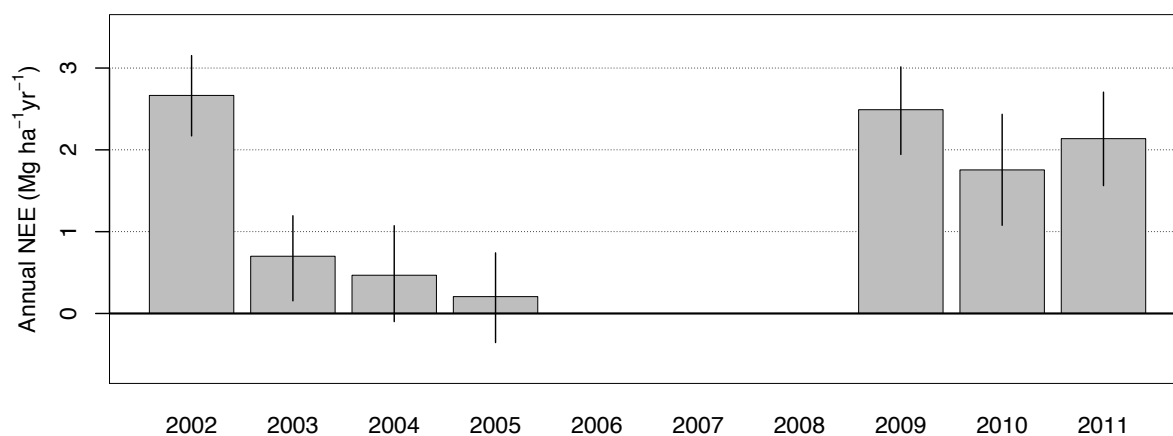
692 **Tables and Figures**

Model Parameters					hourly R <sup>2</sup>	monthly R <sup>2</sup>
$a_0$	$a_1$	$a_2$	$a_3$	$k_{pheno}$		
9.43 (9.30, 9.56)	-1.32 (-1.49, -1.15)	-39.2 (-39.8, -38.6)	760.9 (733.2, 788.6)	0.164 (0.156, 0.171)	0.81	0.59

693 **Table 1. Model parameter values (95% confidence intervals in parentheses) and R<sup>2</sup> fit. Parameters have the following units:  $a_0$ ,  $a_1$ , and**  
 694  **$a_2$ :  $\mu\text{mol-CO}_2 \text{ m}^{-2} \text{ s}^{-1}$ ;  $a_3$ :  $\mu\text{mol-photons m}^{-2} \text{ s}^{-1}$ ;  $k_{pheno}$ : unitless.**

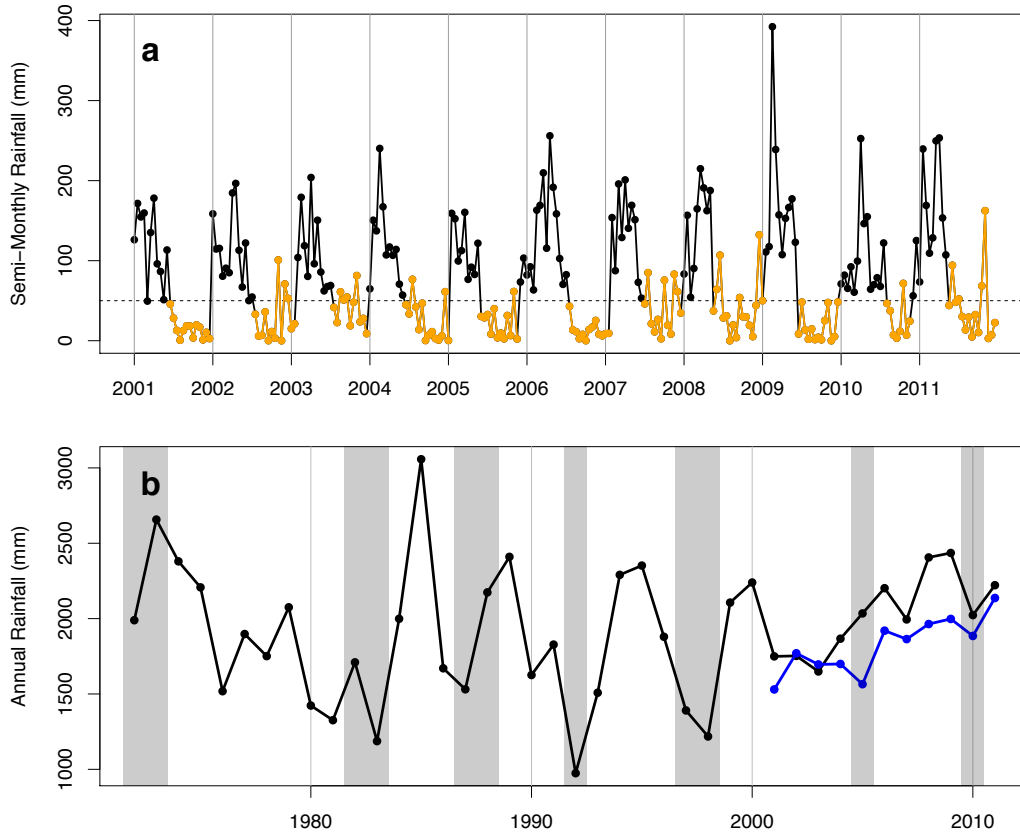
$s_{pheno}$ timing	$k_{pheno}$	hourly R <sup>2</sup>	monthly R <sup>2</sup>
None	-	0.80	0.33
Dry Season	0.117 (0.109, 0.125)	0.80	0.32
June 15 to Sept 14*	0.164 (0.156, 0.171)	0.81	0.59

695 **Table 2.  $k_{pheno}$  parameter values (95% confidence intervals in parentheses) and hourly and monthly model fit associated with various**  
 696 **seasonal timings of the phenology factor variable  $s_{pheno}$ . \*Final model parameterization.**



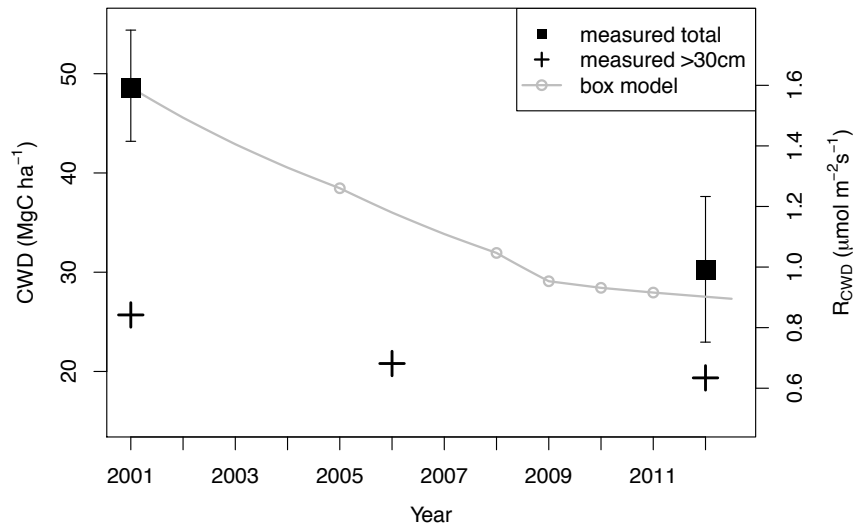
697

698 **Figure 1. Annual sums of NEE in kg/ha/year. Error bars are 95% confidence intervals. Positive values indicate a source of CO<sub>2</sub> to the**  
 699 **atmosphere. Net emission of carbon to the atmosphere during every year in the time series was possibly due to choice of  $u_*^{Th}$  (Fig. S2**  
 700 **for annual NEE time series derived from an alternative choice of flux bias correction).**



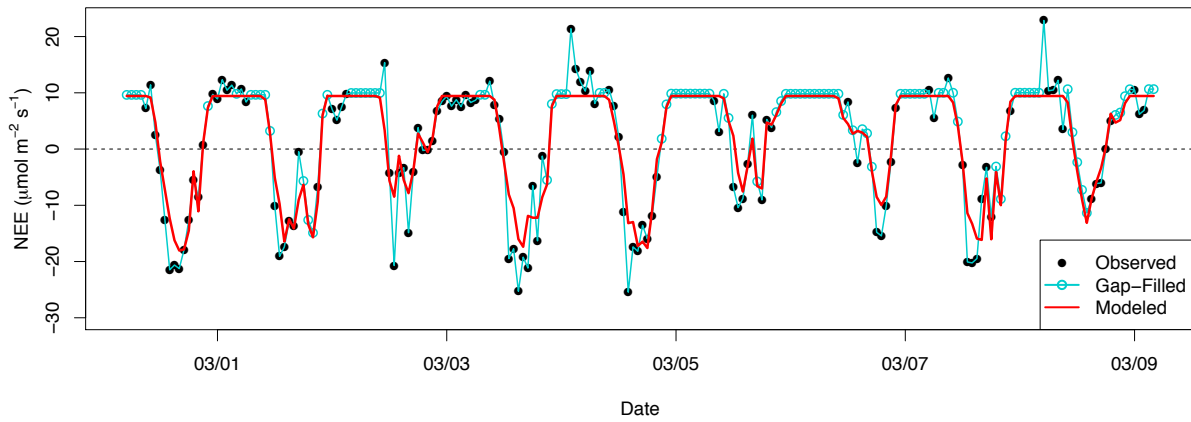
701

702 **Figure 2. (a) Semi-monthly dry season rainfall totals for wet season (black) and dry season (orange). Hourly rainfall was estimated by**  
 703 **objective analysis (Eq. 1) from meteorology stations nearby km67. The horizontal dashed line shows the dry season threshold of 50 mm**  
 704 **per half-month. (b) Yearly totals of rainfall from Belterra INMET station (black), 25 km away from km67, and km67 rainfall**  
 705 **estimated by objective analysis (blue). Recent El Niño anomalies (grey shaded areas) coincide with droughts in the 1990s but not in the**  
 706 **2000s (blue points) at this site, when annual rainfall was within the long-term historical variability.**



707

708 **Figure 3. Measurements of total CWD (black squares with 95% bootstrapped CI error bars) and subsets of CWD  $\geq 30$  cm diameter**  
 709 **(black crosses) show a decrease over time. CWD box model (grey line) also shows a gradual decrease in CWD over time. The initial**  
 710 **condition is the 2001 measurement of CWD; source is input from mortality inferred by biometry census (census times represented by**  
 711 **grey circles); sink is an empirical respiration rate of  $0.124 \text{ yr}^{-1}$  [Pyle et al., 2008]. Left axis shows the CWD respiration flux ( $R_{\text{CWD}}$ )**  
 712 **corresponding to the equivalent amount of CWD on the right axis.**

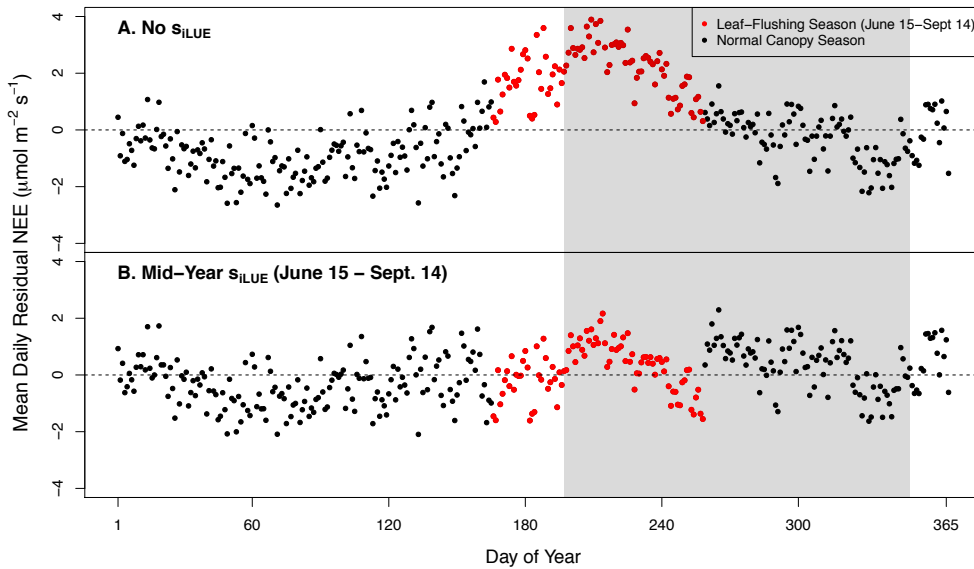


713

714 **Figure 4. Example time series of  $NEE_{obs}$  and  $NEE_{Model}$  for 9 days of the wet season in 2008. Pearson correlation coefficient between**  
 715  **$NEE_{obs}$  and  $NEE_{Model}$  is  $R=0.90$  over the entire 7.5 year time series.**

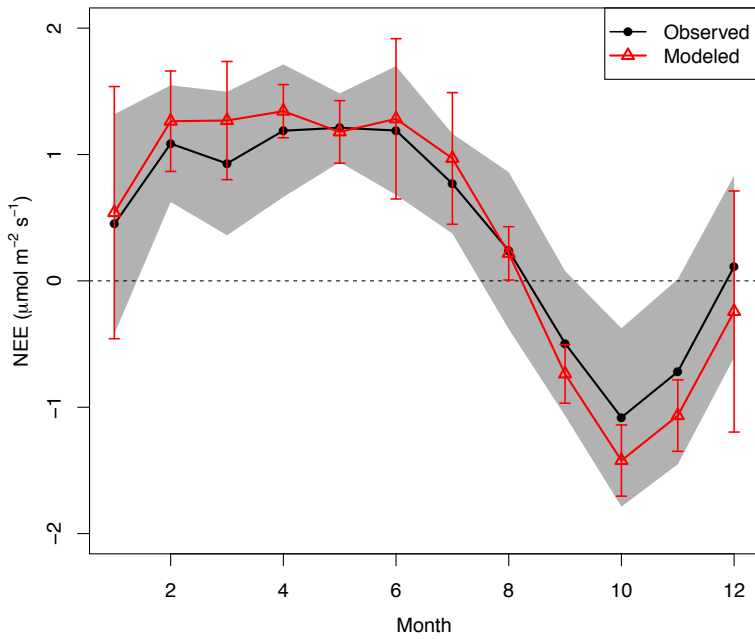
716

717



718

719 **Figure 5. Mean daily data-model residuals averaged over all 7.5 years: (a) lacks an adjustment for phenological change in LUE. Leaf-**  
 720 **flush period only partially overlaps the dry season (grey shaded area). (b) The best-fitting parameterization of the model contained a**  
 721 **mid-year phenology scaling factor ( $1-k_{pheno} \cdot s_{pheno} = 0.84$ ; Table 2), which was asynchronous with the dry season (red points).**



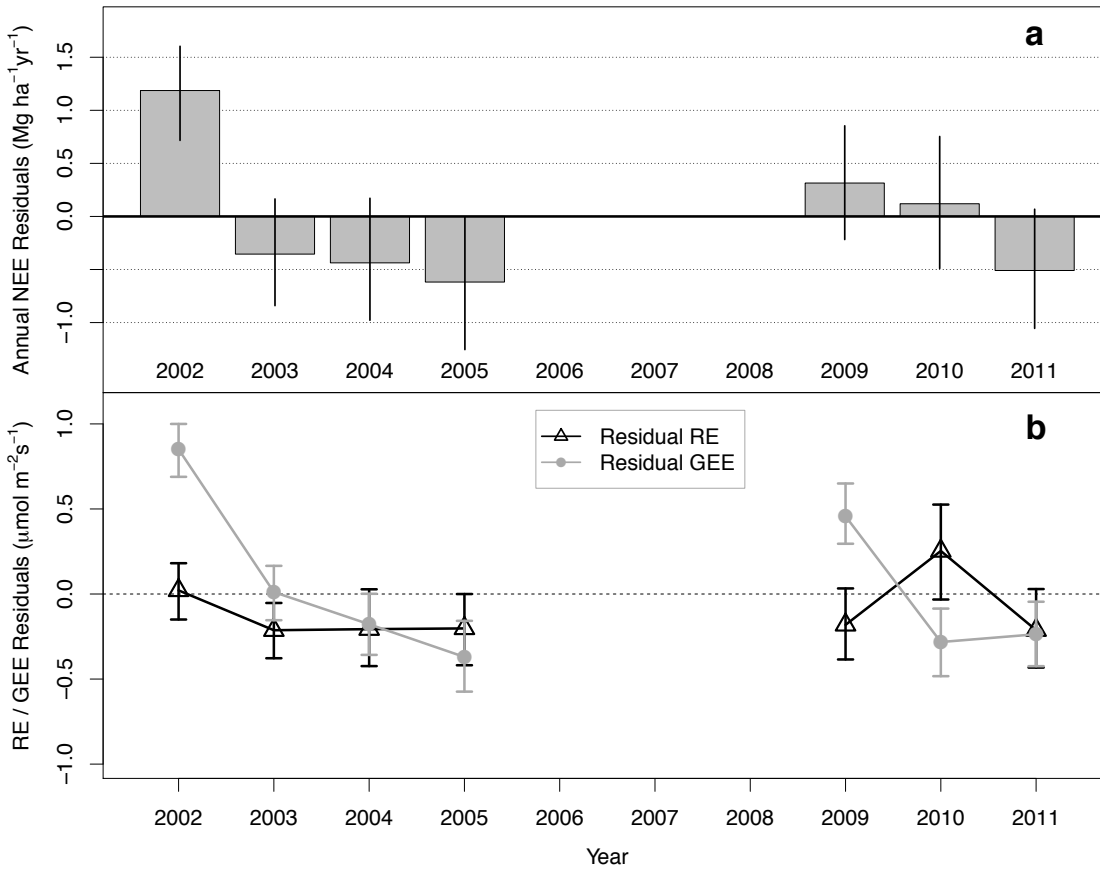
722

723

724

725

**Figure 6. (a) Mean seasonal cycle of  $NEE_{obs}$  (black dots) and  $NEE_{Model}$  (red triangles). Grey shaded areas are standard deviations of interannual variability for the mean  $NEE_{obs}$  for each respective month. Error bars are standard deviations of the interannual variability in monthly mean  $NEE_{Model}$ .**



726

727

728

729

**Figure 7. (a) Annually summed model residuals. Error bars are 95% bootstrapped confidence intervals. Annual residual NEE in 2002 is statistically different from 0 within random NEE measurement error; all other years are not. (b) Residuals of model representation of partitioned GEE (gray circles) and RE (black triangles).**